

Supplementary information

The flow resistance of a circular drop sandwiched between two plates

A. Analytical expression

In the Hele-Shaw approximation, the drag force on a circular drop with radius R sandwiched between two parallel plates with gap h ($h/R \ll 1$) can be calculated analytically. We have to solve the set of equations

$$\nabla p = \mu \left(\nabla^2 \underline{u} - \frac{12}{h^2} \underline{u} \right)$$

$$\nabla \cdot \underline{u} = 0$$

These can be rewritten in terms of the stream function Ψ and the vorticity function Ω as

$$\nabla^2 \Psi = \Omega$$

$$\nabla^2 \Omega = \kappa^2 \Omega$$

where Ψ is defined by $\underline{u} = \nabla \times (\Psi \underline{e}_z)$ and $\kappa^2 = 12/h^2$.

The problem is analysed in cylindrical coordinates with the drop positioned at the origin. At the drop boundary $r = R$ we assume a no-slip boundary condition, and away from the drop the velocity field u_∞ is homogeneous. The complete solution of the flow field around the drop is then given by

$$\Psi(r, \phi) = u_\infty R \sin(\phi) \left\{ \frac{r}{R} - \frac{R}{r} + \frac{2K_1(q)}{qK_0(q)} \left(\frac{K_1(qr/R)}{K_1(q)} - \frac{R}{r} \right) \right\}$$

where K_0 and K_1 are modified Bessel functions of the second kind and $q = 2\sqrt{3}R/h$. From this equation the pressure field can be determined to be

$$p(r, \phi) = p_0 - \mu \kappa^2 u_\infty R \cos(\phi) \left\{ \frac{r}{R} + \frac{R}{r} + \frac{2K_1(q)}{qK_0(q)} \frac{R}{r} \right\}$$

The net force in the direction of the flow on a fluid disc with radius r can subsequently be calculated from

$$F_x = rH \int_0^{2\pi} \underline{e}_r \cdot \left(-p \underline{1} + 2\mu \underline{D} \right) \cdot \underline{e}_x d\phi$$

which for $r = R$ reduces to

$$F_x = \frac{24\pi\mu u_\infty R^2}{h} \left(1 + \frac{2K_1(q)}{qK_0(q)} \right)$$

The results we obtained with this 2D calculation agree well with the two-term approximation as derived by Lee and Fung, which can be used for $(h/R \leq 2.5)$.¹

B. Numerical calculations taking into account the microchannel walls

When the drop size becomes of the order of the finite channel width, the drop blocks a significant fraction of the channel width for flow of the continuous phase. In addition, the no-slip boundary condition at the confining side walls has to be taken into account. Thus, the width of the microchannel becomes the third length scale in the problem, in addition to the drop radius and the channel height. We numerically calculated the flow and pressure fields with an extension of the Hele-Shaw approximation to include the no-slip boundary conditions on the side walls. The problem is reduced to a 2D calculation by averaging the velocity field over the height of the channel. The dimensionless Stokes equations can then be written as

$$\partial_\xi \pi = \{e^2(\partial_\xi^2 + \partial_\eta^2) - 12\} \partial_\eta \psi$$

$$-\partial_\eta \pi = \{e^2(\partial_\xi^2 + \partial_\eta^2) - 12\} \partial_\xi \psi$$

$$\partial_\zeta \pi = 0$$

where π is the dimensionless pressure, ψ the dimensionless stream function, $e = 2h/W$ the aspect ratio of the microchannel, and (ξ, η, ζ) the three dimensionless coordinates. Details of the calculation were previously described in Vanapalli *et al.*² Due to the symmetry of the configuration the calculations are restricted to a single quadrant with $0 < x < W$ and $0 < y < W/2$. After determination of the stream function (Fig. S1A) and the pressure in the channel, the drag force on the drop is calculated by

$$F_{drag} = F_p - F_s - F_b$$

with

$$F_p = -2hW \int_0^W \partial_x p(x, W) dx$$

$$F_s = -4\mu H \int_0^W \partial_y^2 \Psi(x, W) dx$$

$$F_b = 48(\mu W/h)\Psi_W$$

the driving force due to the pressure gradient, and the opposing shear force along the sidewalls and the top and bottom walls, respectively.

The results for channels with various aspect ratios are compared to the expression for an infinitely wide channel (Fig. S2B). Here, we model the drop as a solid disk with a no-slip boundary condition at the drop surface. For small drops, the numerical results nicely coincide with the analytical expression. When the drop size approaches the channel width (as indicated by the vertical lines), the hydrodynamic drag force on the drop diverges due to the pressure build-up.

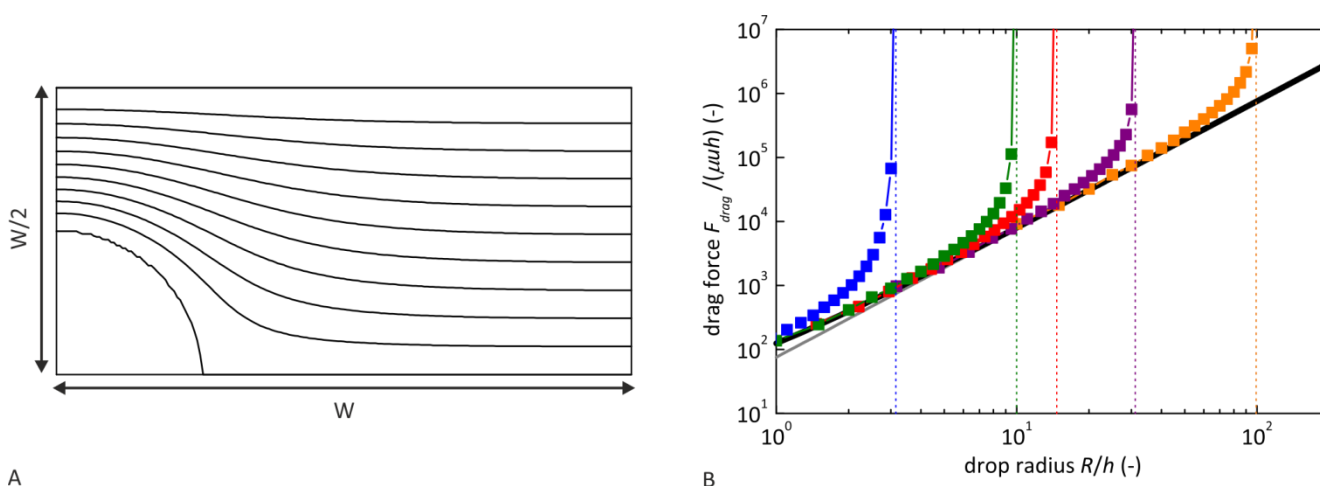


Fig. S1 The drag force on a circular drop. (A) Example of a flow line pattern for a drop with $2R/W = 1/2$. (B) Drag force versus drop radius, as calculated analytically for an infinitely wide channel, i.e. the aspect ratio $e = 2h/W \rightarrow 0$ (thick black line), with scaling arguments for large drops $R \gg h$ (thin gray line), and numerically in a channel with $e = 0.316$ (blue), $e = 0.100$ (green), $e = 0.068$ (red), $e = 0.032$ (purple), and $e = 0.010$ (orange) with a no-slip boundary condition on the drop surface.

Fig. S2A shows an experimental trapping diagram for a channel with $W = 500 \mu\text{m}$ and drop radii R up to $200 \mu\text{m}$. Thus, in these experiments the drop sizes are of the order of the channel width. Using the analytical expression for F_{drag} and plotting it against $F_{el,max}$ in Fig. S2B indicates that the drag force is underpredicted, especially for the larger drops. Using the numerical results for the drag force in Fig. S2C, we now find a much better linear relationship between F_{drag} and $F_{el,max}$. The lack of quantitative correspondence is most probably due to uncertainty in the flow rate (a pressure difference was applied). In addition, for larger trapping forces ($F_{el,max} > 3 \mu\text{N}$) drop deformations start to influence the results significantly.

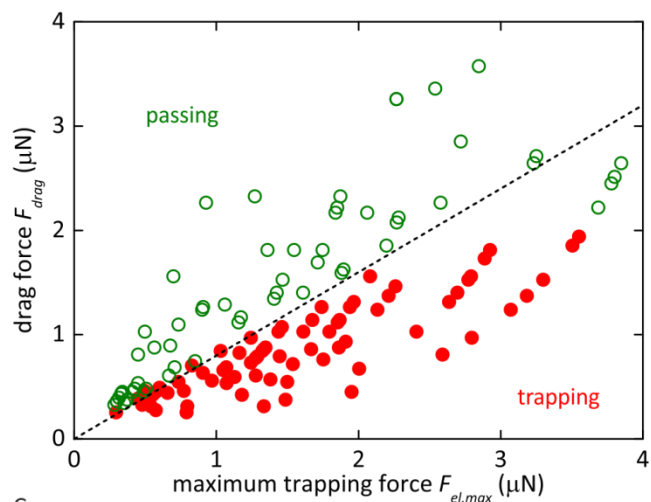
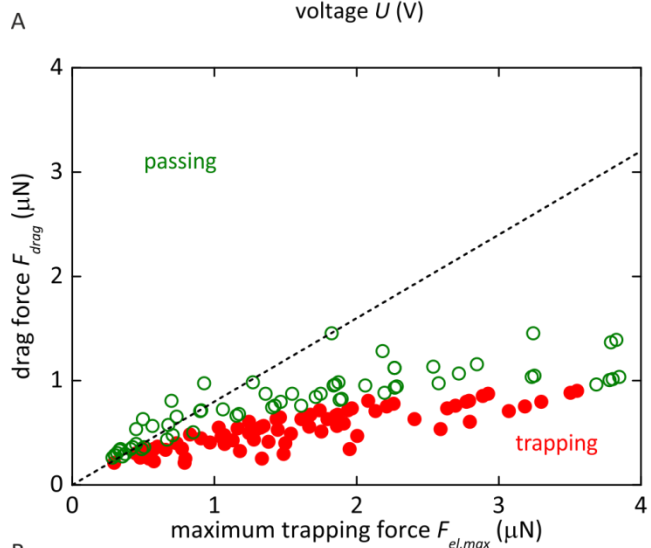
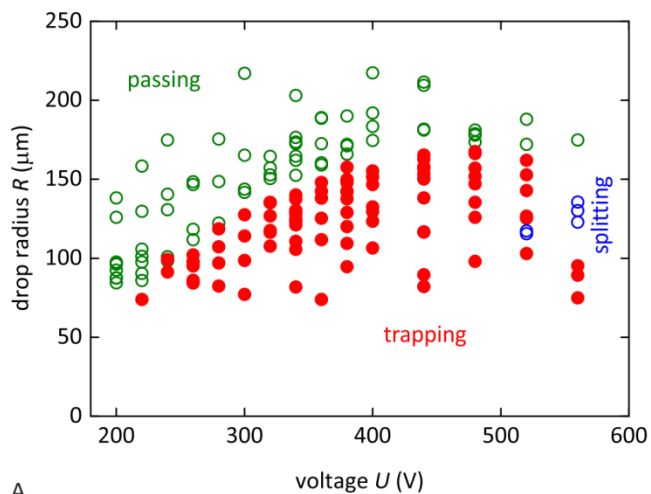
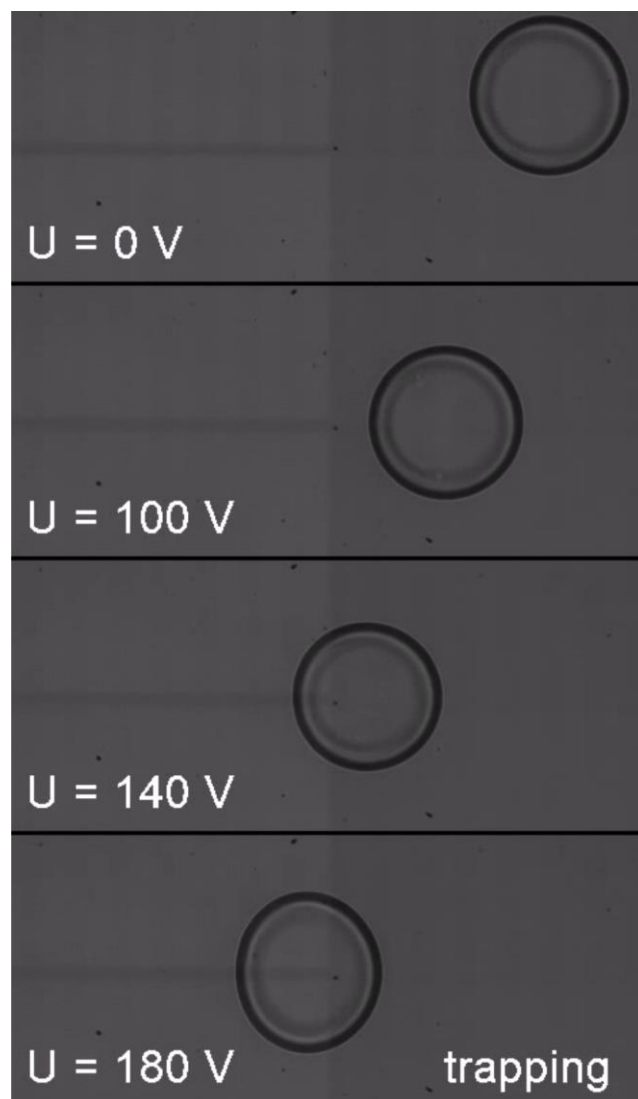
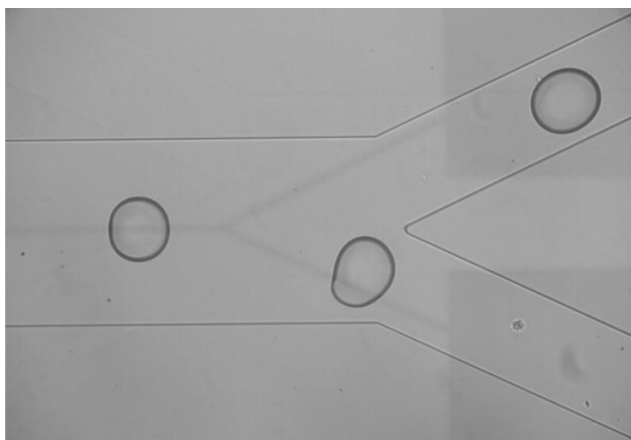


Fig. S2 Experimental results for more narrow channels ($W = 500 \mu\text{m}$). (A) Experimental trapping diagram; depending on applied voltage and drop radius, drops are either being trapped by (red closed symbols), passing (green open symbols), or split by (blue open symbols) the electrodes. (B-C) Drag force versus maximum trapping force for the experimental results in (A). In (B) the drag force is calculated analytically, assuming $2R/W \ll 1$, while in (C) the drag force is calculated numerically, taking into account the finite channel width. The black dotted line is a linear fit to the data in (C) at small trapping force.

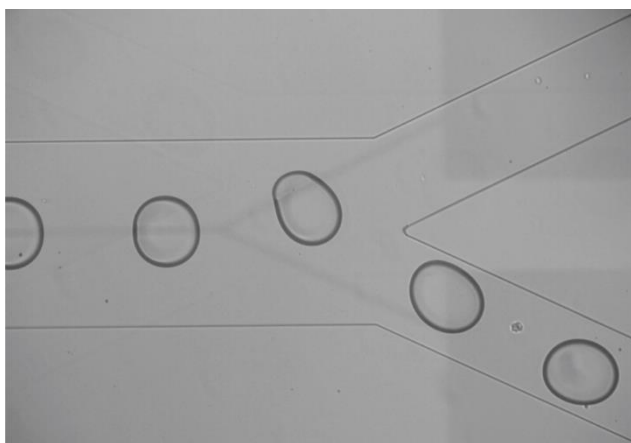
Movies



Movie S1 Real time movie showing the interaction of a drop with co-planar electrodes (with a parallel gap) at various voltages. For $U = 0$ the drop has a constant velocity. For $U = 100 \text{ V}$ and $U = 140 \text{ V}$ the drop is slowed down at the trap, but accelerates back to the initial velocity after leaving the trap. For $U = 180 \text{ V}$ the drop is trapped, and is subsequently released by switching of the voltage.



Movie S2 Alternately sorting of drops. The lower electrode is grounded, while an AC voltage is applied to the upper electrode (225 V, 10 kHz). The same signal is modulated with a square pulse and applied to the middle electrode. When the middle electrode is at 0 V, drops move into the upper branch, and when the middle electrode is at 225 V, drops move into the lower branch. The frequency of the amplitude modulation (11.5 Hz) is chosen such that drops
5 move into the two branches alternately. The flow rates of the mineral oil and the water are 1000 $\mu\text{L/h}$ and 50 $\mu\text{L/h}$, respectively. Drops are formed at a rate of 23 drops per second. The movie is slowed down 20 times.



Movie S3. Selection of a single drop. The lower electrode is grounded, while an AC voltage is applied to the upper electrode (225 V, 10 kHz). The middle electrode is kept at 0 V, causing all drops to move into the upper branch. A single drop is selected to move into the lower branch by giving a short voltage
10 pulse (225 V) to the middle electrode. The flow rates of the mineral oil and the water are 1000 $\mu\text{L/h}$ and 100 $\mu\text{L/h}$, respectively. Drops are formed at a rate of 33 drops per second. The movie is slowed down 20 times.

References

1. J. S. Lee and Y. C. Fung, *J. Fluid Mech.*, 1969, **37**, 657-670.
2. S. A. Vanapalli, A. G. Banpurkar, D. van den Ende, M. H. G. Duits and F. Mugele, *Lab Chip*, 2009, **9**, 982-990.

For streaming channel:

Movie S1

Title: On-demand drop trapping and release in a microchannel using a co-planar electrode configuration.

5 Keywords: microfluidics, microchannel, electrowetting, PDMS, droplet, electrodes, trapping, release, voltage

Movie S2

Title: High-speed sorting of drops in a microchannel using a co-planar electrode configuration.

Keywords: microfluidics, microchannel, electrowetting, PDMS, droplet, electrodes, high-speed, sorting, voltage

10

Movie S3

Title: High-speed selection of a single drop in a microchannel using a co-planar electrode configuration.

Keywords: microfluidics, microchannel, electrowetting, PDMS, droplet, electrodes, high-speed, sorting, voltage